Available online at www.sciencedirect.com
SCIENCE DIRECT®
ELSEVIER
Optics Communications 260 (2006) 542–547
OPTICS COMMUNICATIONS
www.elsevier.com/locate/optcom

# Construction of the refractive index profiles for few-mode planar optical waveguides

Haidong Zhu [a,b,*], Zhuangqi Cao [a], Qishun Shen [a]

[a] Department of Physics, Shanghai Jiao Tong University, 800 Dong Chuan Road, Shanghai 200240, PR China
[b] National Laboratory of High Power Laser and Physics, Shanghai Institute of Optics and Fine Mechanics, Chinese Academy of Sciences, 390 Qing He Road, Box 800-211, Shanghai 201800, PR China

Received 27 July 2005; received in revised form 31 October 2005; accepted 7 November 2005

**Abstract**

We present a nondestructive technique to predict the refractive index profiles of isotropic planar waveguides, on which a thin gold film is deposited to as the cladding. The negative dielectric constant of the metal results in significant differences of effective indices between TE and TM modes. The two polarized modes and a surface plasmon resonance (SPR) with abundant information of the surface index can be used to construct the refractive index profiles of single-mode and two-mode waveguides at a fixed wavelength.


*PACS:* 42.79.Gn; 78.20.Ci; 81.70.Fy

*Keywords:* Refractive index profile; SPR method; Few-mode isotropic waveguides; TE and TM modes

## 1. Introduction

Integrated optical waveguides formed by ion-exchange in glass have attracted considerable interests, due to the low cost of the materials and simplicity of the process in comparison with other techniques. Recently, glass waveguides have been considered to be prime candidates for optical signal processing application in optical amplifier, laser, communication, sensor, power division and other related areas [1–6]. The modeling and fabrication of integrated optical components with well-defined characteristics require an accurate knowledge of refractive index profiles (RIP) of the waveguides. There already exist a number of techniques for the measurement of the index profiles. The most popular methods appear to be the inverse Wentzel–Kramer–Brillouin (IWKB) method [7] and its modified versions [8–10]. Although these methods can give good results in multimode waveguides, there are still some difficult problems in determining the refractive index near the surface of the waveguides. The usual strategies to evaluate the surface index are dependent on the mathematical criteria, rather than the experimental measurements. To determine experimentally the key value, we have employed a SPR technique to obtain a near surface refractive index of a graded-index waveguide, and then improved the IWKB method and the inverse analytical transfer matrix (IATM) method, respectively [11,12]. Numerical examples and experimental results show that the new improved methods can give more accurate results for multimode waveguides than before.

As is well known, a RIP is characterized by its shape, depth, and difference between the peak index and the substrate index, and at least three effective indices are required to give meaningful results. However, a few-mode waveguide can only supply one or two effective indices for one polarized mode at a single wavelength, so one has to resort to other methods to obtain some additional information in predicting its RIP. Recently, much of effort has been devoted to it [13–18]. The outstanding presentations of them are to combine effective indices measured for both of the polarized modes,

* Corresponding author. Tel.: +86 216 991 8287; fax: +86 216 991 8800.
*E-mail address:* hdzhu@mail.siom.ac.cn (H.D. Zhu).

0030-4018/$ - see front matter © 2005 Elsevier B.V. All rights reserved.
doi:10.1016/j.optcom.2005.11.011

and at different wavelength. While, since the differences of effective indices between TE and TM modes are small under the dielectric-cladding condition [19], it is less useful to determine the RIP of few-mode planar waveguides. On the other hand, the technique of combining measurements at different wavelengths requires the accurate knowledge of the material dispersion of both substrate and waveguide.

In this paper, we propose to deposit a thin gold film on the surface of a graded-index isotropic waveguide. As a result, the metal-cladding optical waveguides can accommodate not only the TE and TM modes with significant differences of the effective indices, but also a SPR with abundant information of the surface index. With this nondestructive technique, the index profiles of fewer-mode planar waveguides can be constructed accurately at a fixed wavelength.

## 2. Theory

We first consider a planar waveguides with a graded-index profile of the form,

$$n^2(x) = \begin{cases} n_s^2 + (n_f^2 - n_s^2) f(x/d), & (x > 0), \\ n_m^2, & (x < 0), \end{cases} \tag{1}$$

where $n_f$ and $n_s$ are refractive indices of the surface and the substrate, respectively. As shown in Fig. 1, $f(x/d)$ is the profile function and is assumed to be monotonically decreasing for $x > 0$. $n_m^2$ is the real part of dielectric constant of the metal film. Since the absolute value of the ratio of imaginary to real part of the dielectric constant of metal is small in the visible and near infrared spectrum, we neglect the imaginary part without significant error in the later calculation procedures.

For such a profile, the analytic transfer matrix method gives the following dispersion equations for TE and TM modes [20,21]:

$$\int_0^{x_t} \kappa(x)\,dx + \Phi(s) = \left(m + \frac{1}{2}\right)\pi + \Phi_{mf}^{TE}, \quad m = 0, 1, 2, 3, \cdots, \tag{2}$$

$$\int_0^{x_t} \kappa(x)\,dx + \Phi(s) = \left(m + \frac{1}{2}\right)\pi + \Phi_{mf}^{TM}, \quad m = 0, 1, 2, 3, \cdots, \tag{3}$$

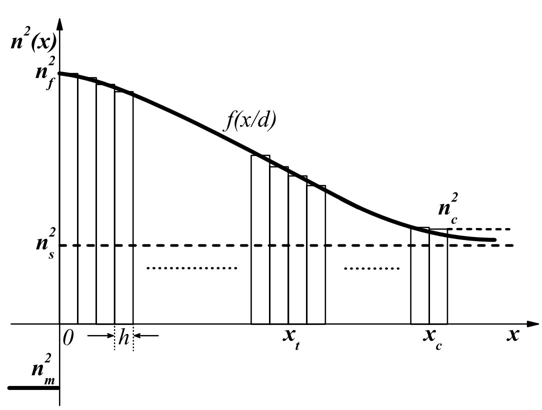


Fig. 1. Plot of planar waveguides with graded-index profile.

where

$$\Phi_{mf}^{TE} = \tan^{-1}\left(\frac{P_m}{\kappa_f}\right),$$

$$\Phi_{mf}^{TM} = \tan^{-1}\left(\frac{n_f^2 P_m}{n_m^2 \kappa_f}\right),$$

$$\kappa(x) = \left[k_0^2 n^2(x) - \beta^2\right]^{1/2},$$

$$\kappa_f = \left(k_0^2 n_f^2 - \beta^2\right)^{1/2},$$

$$P_m = \left(\beta^2 - k_0^2 n_m^2\right)^{1/2},$$

and

$$n(x_t) = \beta / k_0 \tag{4}$$

is the effective index of the guided mode. $\beta$ is the corresponding propagation constant, $k_0 = 2\pi/\lambda$ is wavenumber with wavelength $\lambda$ in free space, and $x_t$ is the turning point. $x_c$ is the truncation point, which is determined by a prescribed accuracy, and we assume $n(x_c) = n_c$. The function $\Phi(s)$ is the phase contribution of the sub-waves reflected from every interface between the neighboring section layers. The detailed explanations are available in [20,21]. Combined Eqs. (2) and (3) with (4), the propagation constants of the TE and TM guided modes can be determined accurately.

In the visible and near infrared spectrum, we have $n_m^2 < 0$ and $|n_m^2| \gg n_f^2$, and the significant differences of the effective indices between TE and TM modes are thus exhibited [19]. In addition, a SPR can be excited in the metal-cladding waveguides. The analysis and calculations in [11,12] show that the special feature of the SPR can be used to evaluate an equivalent refractive index $n_{eq}$, which is much closer to the surface index than that of the first guided mode. The equivalent refractive index $n_{eq}$ is described by the following well known dispersion equation [22],

$$\frac{\beta_{SPR}}{k_0} = \left(\frac{n_m^2 n_{eq}^2}{n_m^2 + n_{eq}^2}\right)^{1/2}. \tag{5}$$

In experimental measurements, the propagation constant $\beta_{SPR}$ can be determined in the Kretschmann configuration at the largest resonance angle. As a result, if $n_m^2$ is known, the equivalent index with respect to SPR, $n_{eq}$ can then be calculated from Eq. (5).

In our previous work [23], the refractive index distributions $n(x)$ can be constructed by IATM method with the one polarized mode. Here, we extend it to reconstruct the RIP of graded-index isotropic waveguide with both TE and TM guided modes, and the SPR.

During above the reconstruction, it relates to eight equations presented in [11]. For integrity of this paper, we give them out in detail. According to the ATM method [20], the SPR mode dispersion equation is as follows:

$$\begin{bmatrix} -\frac{P_m}{n_m^2} & 1 \end{bmatrix} \left[\prod_{i=0}^{l} M_i\right] \begin{bmatrix} 1 \\ -\frac{P_c}{n_c^2} \end{bmatrix} = 0, \tag{6}$$

Table 1
Numerical results of equivalent and effective indices, $n_{eq}$ and $N$, for three typical distributions

| Profile | $n_{eq}$ | $N_0^{TE}$ | $N_1^{TM}$ | $N_1^{TE}$ | $N_2^{TM}$ |
|---|---|---|---|---|---|
| Exponential | 1.5546 | 1.5222 | 1.5159 | 1.5067 | 1.5048 |
| Slow Fermi | 1.5600 | 1.5325 | 1.5241 | 1.5084 | 1.5048 |
| Gaussian | 1.5606 | 1.5275 | 1.5163 | None | None |

where

$$M_i = \begin{bmatrix} \cosh(\alpha_i h) & -\frac{n_i^2}{\alpha_i}\sinh(\alpha_i h) \\ -\frac{\alpha_i}{n_i^2}\sinh(\alpha_i h) & \cosh(\alpha_i h) \end{bmatrix}, \quad (i = 0, 1, 2, \ldots l) \tag{7}$$

and

$$\alpha_i = [\beta^2 - k_0^2 n^2(x_i)]^{1/2},$$
$$P_c = \left(\beta^2 - k_0^2 n_c^2\right)^{1/2}. \tag{8}$$

Obviously, Eq. (6) can be reduced to

$$\begin{bmatrix} -\frac{P_m}{n_m^2} & 1 \end{bmatrix} \begin{bmatrix} 1 \\ -\frac{P_{eq}}{n_f^2} \end{bmatrix} = 0, \tag{9}$$

where

$$P_{eq} = P_f, \tag{10}$$
$$P_i = \alpha_i \frac{n_{i+1}^2 \alpha_i \sinh(\alpha_i h) + n_i^2 P_{i+1} \cosh(\alpha_i h)}{n_{i+1}^2 \alpha_i \cosh(\alpha_i h) + n_i^2 P_{i+1} \sinh(\alpha_i h)}, \quad (i = 0, 1, 2, \ldots l) \tag{11}$$
$$P_{l+1} = P_c. \tag{12}$$

$P_{eq}$ is characterized by the equivalent dielectric constant $n_{eq}^2$, whose expression is

$$P_{eq} = \left(\beta^2 - k_0^2 n_{eq}^2\right)^{1/2}. \tag{13}$$

Subsequently, the practical calculations for predicting the RIP of graded-index isotropic waveguides can be completed with the following four steps.

1. With the metal-cladding waveguides and the conventional prism coupling technique [24], measure the effective index of the SPR mode $\beta_{SPR}/k_0$, and two sets of effective indices for TE and TM guided modes, $\{N_m^{TE}\}$ and $\{N_{m+1}^{TM}\}$, and then calculate the equivalent index $n_{eq}$ by substituting $\beta_{SPR}/k_0$ to Eq. (5).
2. Choose an initial surface refractive index $n_0$ ($n_0 > n_{eq}$) and combine the measured effective indices of both of the polarized modes to construct the index profile $n(x)$ by the conventional IATM method [23].
3. With the obtained index profile $n(x)$ from step (2), using Eqs. (5) and (10)–(13), we can calculate a new equivalent index $n'_{eq}$, and reset a new surface index as $n_0 + (n_{eq} - n'_{eq})$.
4. Use the newly obtained surface index $n_0$ to reconstruct a new RIP from step (2). Subsequently, repeat step (3) till the value of $n_0$ converges. Then the final RIP of the waveguide is determined.

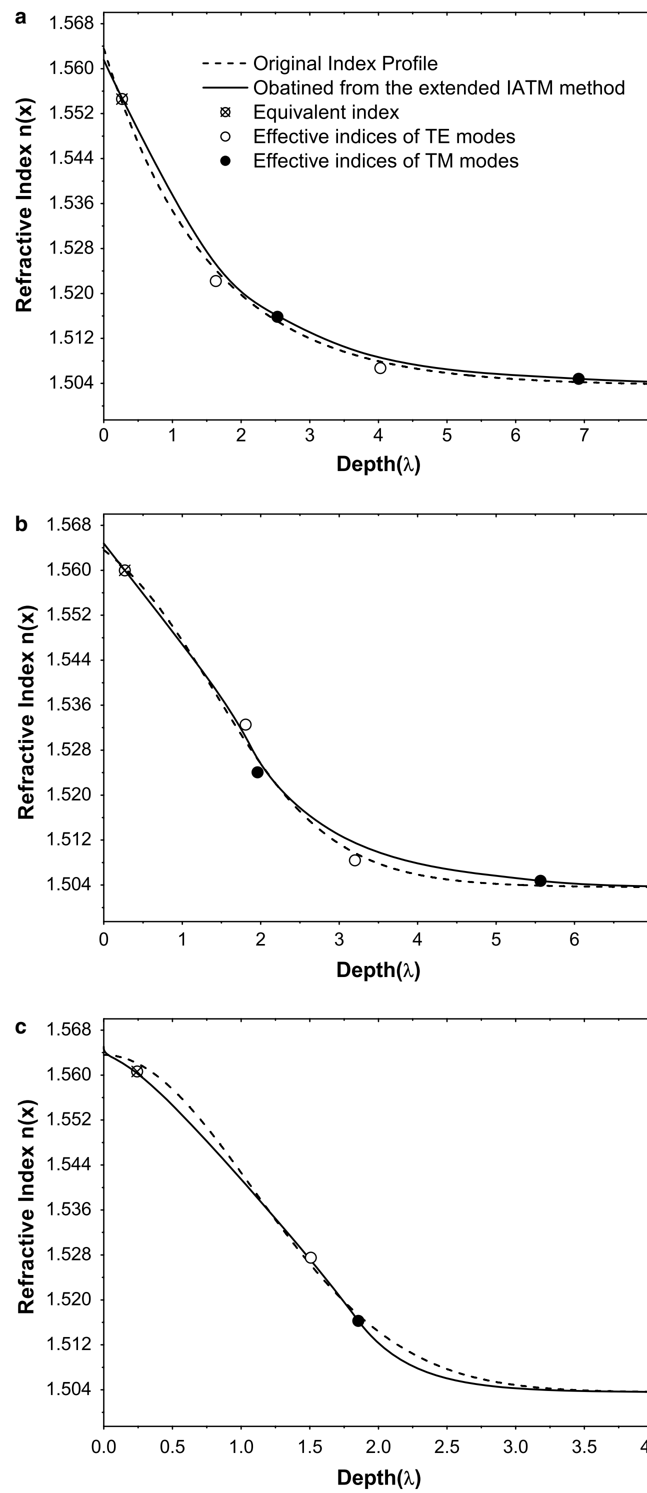


Fig. 2. Numerical results of the profiles for few-mode waveguides in the extended IATM method: (a) exponential profile, (b) slow Fermi profile, (c) Gaussian profile.

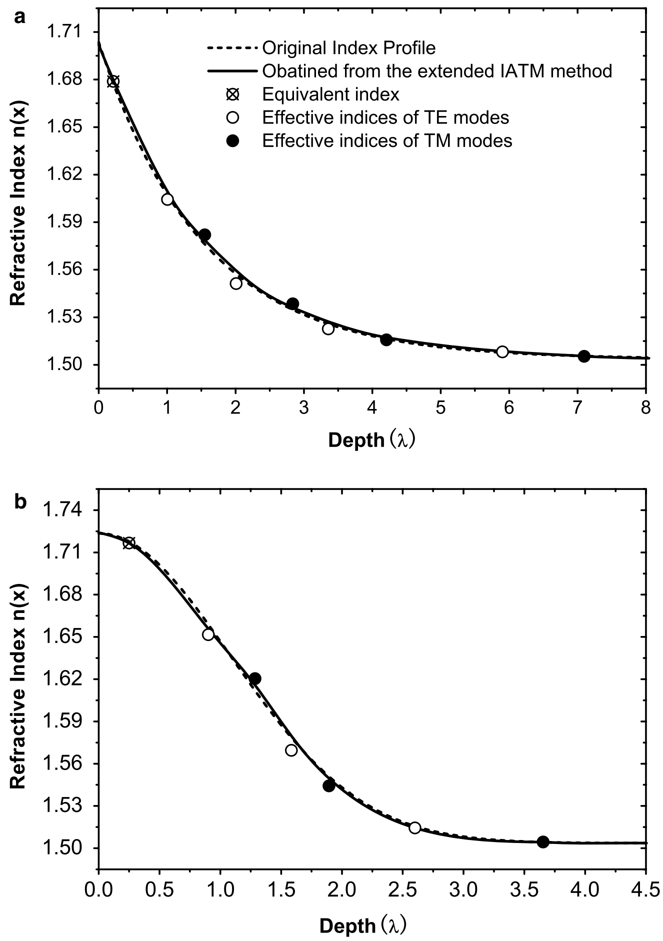


Fig. 3. Numerical results of the profiles for multimode waveguides in the extended IATM method: (a) exponential profile, (b) Gaussian profile.

From the method presented above, using Eqs. (5) and (10)–(13) and the conventional IATM method, the RIP near and far from the surface of isotropic waveguides can be constructed accurately. Therefore, under the metal-cladding condition, we make full use of the TE and TM modes with significant differences of the effective indices and the SPR with abundant information of the surface index to construct the RIP of the few-mode planar waveguides at a fixed wavelength. It is obviously found that the newly presented inverse method named extended IATM method is especially suitable for a few-mode isotropic waveguides.

## 3. Numerical results

To test the reliability of the extended IATM method, we carry out numerical simulations for three typical profiles with exponential, slow Fermi, and Gaussian distributions, respectively. Their expressions are presented as follows, where $x$ is in micrometer and $x \geqslant 0$:

(a) Exponential index profile:

$$n(x) = 1.5036 + 0.06\exp(-x/2), \tag{14}$$

(b) Slow Fermi index profile:

$$n(x) = 1.5036 + \frac{0.06}{1 - \exp(-2) + \exp(x - 2)}, \tag{15}$$

(c) Gaussian index profile:

$$n(x) = 1.5036 + 0.06\exp(-x^2/4). \tag{16}$$

The parameters are $n_{\mathrm{m}}^2 = -68$ at $\lambda = 1.31$ μm, the width of the sublayer $h = 0.5$ nm, and $x_c = 5$ μm in the calculation procedures. With the same surface index $n_f = 1.5636$, we first calculate the effective indices of above profiles with Eqs. (2)–(4), and the equivalent indices with Eq. (5). The calculated results are listed in Table 1 and the effective indices of the SPR mode $\beta_{\mathrm{SPR}}/k_0$ are 1.5845, 1.5898 and 1.5904, respectively. The extended IATM method is then used to construct the three index profiles. The predicted RIP and their original ones are shown in Fig. 2. It is found that the results obtained from the extended IATM method are consistent with the original profiles.

To illustrate further the universality of our method for multimode isotropic waveguides, other two typical index profiles with exponential and Gaussian distributions, which can accommodate four and three guided modes respectively, are considered in the same method. The equations are

(a) Exponential index profile:

$$n(x) = 1.5036 + 0.2\exp(-x/2), \tag{17}$$

(b) Gaussian index profile:

$$n(x) = 1.5036 + 0.22\exp(-x^2/4). \tag{18}$$

As illustrated in Fig. 3, the reconstructed RIP with the extended IATM method agree with their original. From Figs. 2 and 3, we easily discover our presented inverse method can predict not only the RIP of few-mode isotropic waveguides but also multimode ones. However, in order to reduce calculations, we prefer to do it with the one polarized mode for multimode waveguides.

## 4. Experimental results

To verify the present method experimentally, we prepare three pieces of $Ag^+$–$Na^+$ ion-exchanged isotropic wave-

Table 2
Measured equivalent and effective indices, $n_{\mathrm{eq}}$ and $N$, for three ion-exchanged BK7 glass waveguides before and after deposition gold film

| Sample | Before deposition | | | | After deposition | | | | |
|---|---|---|---|---|---|---|---|---|---|
| | $N_0^{\mathrm{TE}}$ | $N_0^{\mathrm{TM}}$ | $N_1^{\mathrm{TE}}$ | $N_1^{\mathrm{TM}}$ | $n_{\mathrm{eq}}$ | $N_0^{\mathrm{TE}}$ | $N_1^{\mathrm{TM}}$ | $N_1^{\mathrm{TE}}$ | $N_2^{\mathrm{TM}}$ |
| A | 1.5177 | 1.5175 | None | None | 1.5297 | 1.5170 | 1.5136 | None | None |
| B | 1.5350 | 1.5348 | 1.5145 | 1.5142 | 1.5664 | 1.5347 | 1.5284 | 1.5140 | 1.5080 |
| C | 1.5289 | 1.5286 | 1.5115 | 1.5113 | 1.5425 | 1.5287 | 1.5232 | 1.5109 | 1.5076 |

guides in BK7 glass. The bulk refractive index of the glass substrates is 1.5036 at $\lambda = 1.31$ μm. Purely thermal ion exchange is carried out at $T = 345$ °C with the melt concentration 9.1 wt% $AgNO_3$ and 90.9 wt% $NaNO_3$. Three samples are fabricated with different exchange time: sample A, 60 min; sample B, 90 min; and sample C, 120 min. With the conventional *m*-line technique [24], we preform the measurements before and after a gold film deposition on the surface of the samples, respectively. The obtained results are listed in Table 2. It is found that, for the waveguides after the gold film deposition, the differences of the effective indices between the two polarized modes are much larger than those of the case with air cladding, and the equivalent indices with respect to the SPR are much closer to the surface indices than those of the first guided mode. Therefore, we obtain more valuable information to predict the index distributions of the waveguides than before.

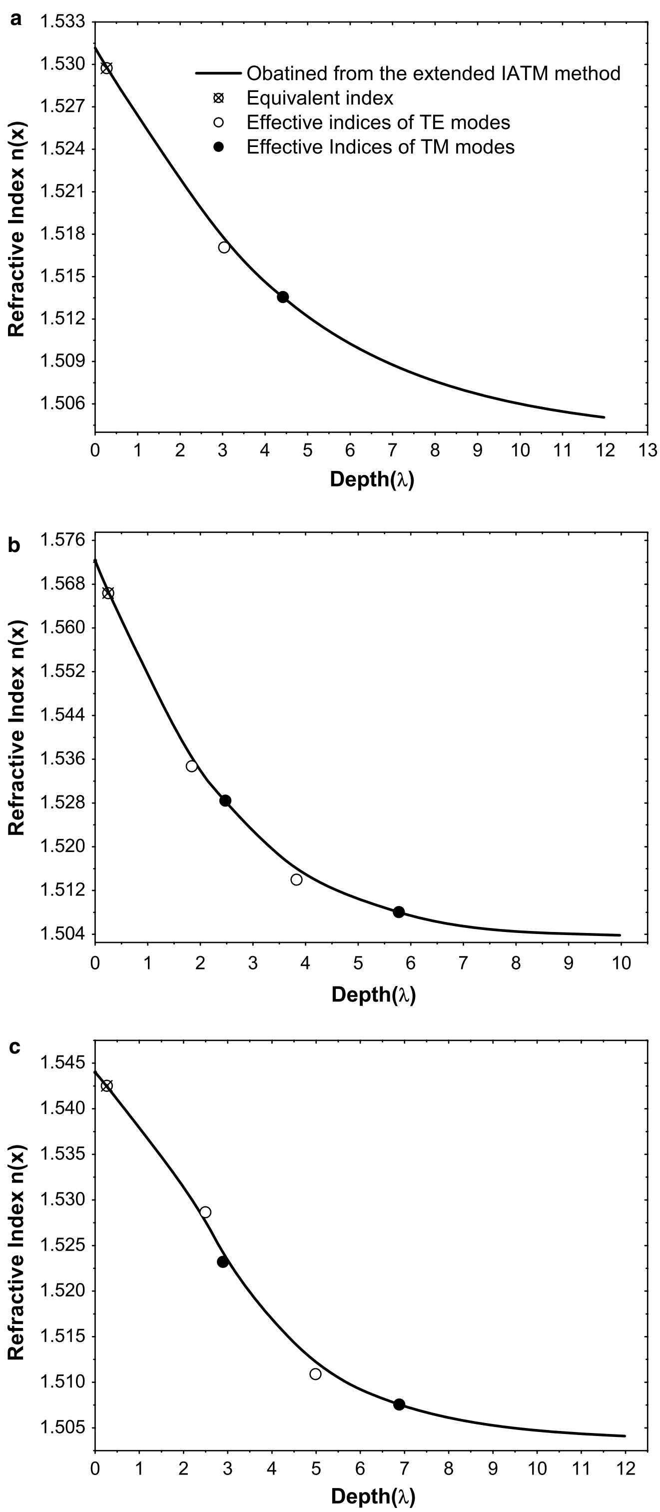


Fig. 4. Experimental results of the three ion-exchanged waveguides obtained from the extended IATM method: (a) 60 min, (b) 90 min, (c) 120 min.

The gold film ($d = 32$ nm, $n_m^2 = -66.49$) is deposited on the surface of the samples by vacuum sputtering at room temperature, whose thickness and the dielectric constant of the thin metal film are determined by Chen's method [25]. Similar to the previous work [11,12], to enhance the coupling, a matching liquid of the refractive index just equal to that of the prism is used to fill the gap between the prism and the gold film. As a test, after removing the thin gold film on the samples with an aqua-regia solution, we check the bare waveguides again and do not find changes of the effective indices within the experimental errors.

Finally, with the measured values and the extended IATM method, index profiles of the three samples are successfully constructed. The results are shown in Fig. 4. It can be seen that the constructed profiles are in good agreement with the physical prediction using ion-exchanged technique [26]. However, we also found the longer exchange time did not result in index change inside deeper substrate for the three samples. The main reasons for the unusual phenomenon are no enough convection and inhomogeneous concentration in the melts. In the later research, we should improve our experimental techniques to avoid it.

## 5. Discussion and conclusion

A nondestructive and simple technique has been developed to determine the RIP of graded-index isotropic waveguides. With the presented technique, more valuable and additional information of the RIP, which is based on the characteristics of the metal-cladding optical waveguides, can be obtained than before. Numerical and experimental results have shown that the extended IATM method is accurate and more suitable for predicting the RIP of few-mode isotropic waveguides than before. However, some waveguides are birefringent or do not support both TE and TM modes. For such waveguides, we have to resort to other techniques to solve it.

## Acknowledgements

The work was supported by the National Natural Foundation of China (No. 60237010), and the Exploring Foundation of National High-Tech ICF Committee of China (No. 2003AA84ts17).

## References


[1] F. Gardillou, L. Bastard, J.E. Broquin, Appl. Phys. Lett. 85 (2004) 5176.
[2] P. Madasamy, S. Honkanen, D.F. Geraghty, N. Peyghambarian, Appl. Phys. Lett. 82 (2003) 1332.
[3] P. Madasamy, B.R. West, M.M. Morrell, D.F. Geraghty, S. Honkanen, N. Peyghambarian, Opt. Lett. 28 (2003) 1132.
[4] R. Yin, X.Q. Jiang, J.Y. Yang, M.H. Wang, J. Opt. Soc. Am. B 19 (2002) 1301.
[5] C.R. Lavers, K. Itoh, S.C. Wu, M. Murabayashi, I. Mauchline, G. Stewart, T. Stout, Sens. Actuators B 69 (2000) 85.
[6] A. Kaplan, S. Ruschin, IEEE J. Quantum Electron. 37 (2001) 1562.
[7] J.M. White, P.F. Heidrich, Appl. Opt. 15 (1976) 151.
[8] R. Oven, S. Batchelor, D.G. Ashworth, D. Gelder, J.M. Bradshaw, Electron. Lett. 31 (1995) 229.
[9] K.S. Chiang, J. Lightwave Technol. 3 (1985) 385.
[10] P. Hertel, H.P. Menzler, Appl. Phys. B 44 (1987) 75.
[11] H.D. Zhu, Y. Ding, Z.Q. Cao, Q.S. Shen, Opt. Commun. 246 (2005) 331.
[12] H.D. Zhu, Z.Q. Cao, Q.S. Shen, Appl. Opt. 44 (2005) 3174.
[13] B. Pantchev, Z. Nikolov, IEEE J. Quantum Electron. 29 (1993) 154.
[14] S. Batchelor, R. Oven, D.G. Ashworth, Opt. Commun. 131 (1996) 31.
[15] K.S. Chiang, C.L. Wong, H.P. Chan, Y.T. Chow, J. Lightwave Technol. 14 (1996) 827.
[16] R. Oven, S. Batchelor, D.G. Ashworth, IEE Proc. Optoelectron. 144 (1997) 213.
[17] Alexei A. Podviaznyi, Dmitry V. Svistunov, Opt. Commun. 201 (2002) 325.
[18] K.S. Chiang, C.L. Wong, S.Y. Cheng, H.P. Chan, J. Lightwave Technol. 18 (2000) 1412.
[19] I.P. Kaminow, W.L. Mammel, H.P. Weber, Appl. Opt. 13 (1974) 396.
[20] Z.Q. Cao, Y. Jiang, Q.S. Shen, Y.L. Chen, J. Opt. Soc. Am. A 16 (1999) 2209.
[21] Z.Q. Cao, Q. Liu, Y. Jiang, Q.S. Shen, X.M. Dou, J. Opt. Soc. Am. A 18 (2001) 2161.
[22] E. Kretschmann, Z. Physik 241 (1971) 313.
[23] Y. Ding, Z.Q. Cao, Q.S. Shen, Opt. Quantum Electron. 36 (2004) 489.
[24] R. Ulrich, R. Torge, Appl. Opt. 12 (1973) 2901.
[25] W.P. Chen, J.M. Chen, J. Opt. Soc. Am. 71 (1981) 189.
[26] R.V. Ramaswamy, R. Srivastava, J. Lightwave Technol. 6 (1988) 984.